Proceedings of the Asia-Pacific Advanced Network ***2013*** *v. 35, p. 49-61.*
http://dx.doi.org/10.7125/APAN.35.6
ISSN 2227-3026

Using the Short-Wave Infrared for Nocturnal Detection of Combustion Sources in VIIRS Data

Mikhail Zhizhin[1]*, Christopher D. Elvidge[2], Feng-Chi Hsu[1] and Kimberly E. Baugh[1]
[1] Cooperative Institute for Research in Environmental Sciences
University of Colorado, Boulder, Colorado, USA

[2] NOAA National Geophysical Data Center NOAA
325 Broadway E/GC2, Boulder, Colorado, USA

E-mail: Mikhail.Zhizhin@noaa.gov, Chris.Elvidge@noaa.gov, Feng.C.Hsu@noaa.gov, Kim.Baugh@noaa.gov
* Author to whom correspondence should be addressed; Tel.: +1-303-497-6385

Abstract:

Night-time images from the SNPP satellite VIIRS scanning radiometer in visible and infrared spectral bands provide invaluable data for detection and characterization of natural and technological combustion sources on the surface of the Earth, such as forest fires, gas flares, steel mills or active volcanoes. The presence of sub-pixel hot infrared (IR) emission sources can be readily detected at night in 1.6 micron near-infrared M10 channel. Their temperature and radiant heat intensity can be estimated by fitting of the Planck black-body spectral curve to the observed radiances of VIIRS infrared M-channels out to 4 um. VIIRS instrument is sensitive to the IR sources over a wide range of temperatures. This method can discriminate low temperature sources such as volcanoes and forest fires from the high temperature gas flares with 300 m average location error. The processing includes correction for panoramic “bow-tie” effect and filtering of the false detections resulting from sensor bombardment by the cosmic rays, especially at the aurora rings and at the South Atlantic anomaly. False detections can be removed by correlating of the observed bright spots in M10 channel with other infrared and the visible day-night band. NGDC NOAA provides global daily detection products for thousands of IR sources as KMZ vector maps and as CSV tables.

Keywords: remote sensing, nocturnal detection, infrared combustion sources, gas flares, biomass burning, active volcanoes.

1. Introduction

Detection of the infrared combustion sources on the Earth surface from satellites is important to the study of biomass and gas flare burning, which result in greenhouse gas emissions volumes large enough to affect ecology and global climate [1,2]. Although it is possible to detect some combustion sources during the day, nocturnal observations are advantageous since the radiant emissions can be observed without solar contamination.

Satellite detection of hot sources on the Earth had been standard practice since 1980s. Thermal channels originally designed to identify cloud-contaminated pixels and evaluate the radiant contribution from water vapor also showed the ability to detect pixels with high temperature sources. Dozier et al. [3,4] demonstrated that by taking the difference of radiative brightness temperature of NOAA AVHRR channels 3 (MIR) and 4 (TIR) whose wavelength centered at 4um and 11um respectively, it is possible to calculate the temperature of heat source and its portion of the pixel. The method only works for pixels where the hot source is detected in both spectral bands, which is a rare occurrence in the 11 um channel. Identifying pixels with hot sources based on the brightness temperature difference between a 4 um and an 11 um channel emerged as the primary method for generating fire products from both AVHRR and MODIS data [5,6,7].

The VIIRS is unique among satellite sensors for its collection of three near-and-short wave infrared bands at night. These are designed as daytime imaging bands. At night they collect data that are remarkable for their ability to detect combustion sources. In this paper we present a novel multi-spectral method for detection of nocturnal IR sources on the Earth and determine their temperature, portion of pixel, radiant heat intensity and radiant heat using up to six spectral bands spanning the visible to mid-infrared.

2. Method

The set of VIIRS radiometer moderate resolution infrared channels providing data at night is shown in Table 1. It is different from the daytime data set because some of the channels are not collected at night to save satellite communications bandwidth and ground processing. However, comparing the available channel bandwidths with a Planck black body radiation curve of the burning methane with the temperature 2223 K (Figure 1) allows one to conclude that anomalously bright pixels detected at night in 1.6 micron near-infrared M10 channel contain hot objects that are IR emitters.

The Planck law describes the radiation emitted by a black body in thermal equilibrium at a definite temperature as a function of electromagnetic wavelength. The function for the Planck curve can be written as:

$$R(\lambda, T) = \varepsilon \frac{2hc^2}{\lambda^5} \frac{1}{e^{\frac{hc}{\lambda k_B T}} - 1} \quad (1)$$

where R is spectral radiance of the surface of the black body (W/m^2/sr/um), T is its absolute temperature (K), λ is the wavelength (um), k_B is the Boltzmann constant, h is the Planck constant, and ε is the emissivity scaling factor to compensate for graybody behavior.

2.1. The M10 hot pixel detector

Distribution of the central wavelengths for the VIIRS sensor M-channels at night are suitable for detection and measurement of radiant features of flares in the temperature range from 600 K to 3000 K. Among all the VIIRS M-bands the spectral channel M10 has proven to be the most informative for combustion source detection at night due to the well-positioned central wavelength of 1.6 um and the high signal to noise ratio (Figure 2). In contrast, the daytime the M10 channel data are contaminated by sunlight rendering it unusable for fire detection.

In the single-band detector of the combustion sources the signal above the noise level threshold THR_{M10} = mean(*M10*) + 6 × std(*M10*) is reported as a possible IR source. Here the mean and the standard deviation are calculated for the "noisy" part of the M10 channel image, which includes pixels with brightness below 100 DNs (digital numbers) but excludes sunlit part of the image near terminator defined by solar zenith angle less than 95 deg.

2.2. Are the pixels hot in other spectral bands

The next processing step is to examine the M10 hot pixels to determine if they are also hot in other spectral bands. This is done for two reasons:

- To assemble a set of multispectral radiances suitable for analysis of temperature and source size (power, volume of burned material…).
- Filtering to remove false detections.

In the multiband detector independent thresholds are used for all M-bands to detect IR signal above noise level. For bands M7, M8 and M10 the thresholds are based on N-sigma rule for average and standard deviations calculated over the whole image, similar to calculation of the THRM10 threshold.

Table 1. VIIRS radiometer visible and infrared channels available at night

VIIRS band name	Central wavelength (µm)	Bandwidth (µm)	Wavelength range (µm)	Band type
DNB	0.7	0.4	0.5-0.9	Visible
M7	0.865	0.039	0.846 - 0.885	NIR
M8	1.24	0.02	1.23 - 1.25	SWIR
M10	1.61	0.06	1.58 - 1.64	
M12	3.7	0.18	3.61 - 3.79	MWIR
M13	4.05	0.155	3.97 - 4.13	
M14	8.55	0.3	8.4 - 8.7	LWIR
M15	10.763	1.0	10.26 - 11.26	
M16	12.013	0.95	11.54 - 12.49	

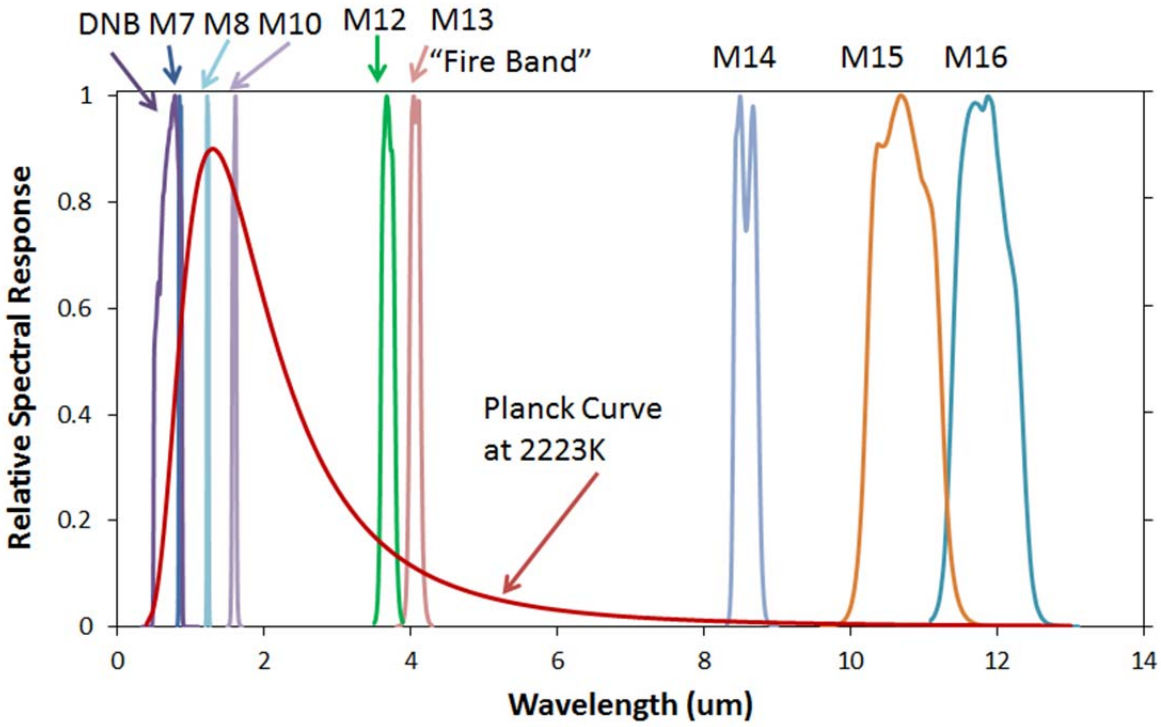

Figure 1. Comparison of a Planck curve (red) from a hot object versus the VIIRS spectral bands that collect at night. 2223K is reported as the combustion temperature of pure methane burning in air.

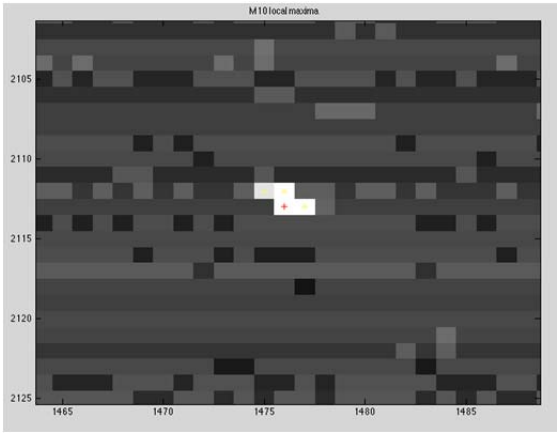

Figure 2. Point IR source detected by several pixels in VIIRS M10 channel.

For bands M12 and M13 the detection threshold is dynamically updated in a moving window 11x11 pixels centered at each M10 local maximum. In that case the M12 and M13 background signal statistics are estimated only for pixels inside the moving window with radiance below the noise level in the M10 band (with brightness < THRM10). Difference between the observed M12 and M13 radiances for the detected IR source and the mean values of the M12 and M13 signal in the noisy part of the moving window serves as an estimate of the IR source brightness in this spectral bands and it will be used later for the Planck black body curve fitting.

To match the hot spots detected in the M10 band with the bright night time lights observed in the visible DNB band, we have to take into account difference in the M10 and DNB image geometry. First, we search for a DNB pixel in the same scan line, as the M10 hot spot, using geolocation data (latitudes and longitudes of pixel centers) for both images. Then we search for the local maxima in a square 11x11 pixel window centered at that DNB pixel. Finally, we assign to the M10 hot spot the nearest DNB local maximum found in that window (if any).

2.3 Filtering to remove noise

False single-band detections occur when the spacecraft flies through energetic particle precipitation regions. Here there are random hits on detectors by cosmic rays from above. These false detections are most frequently observed in the South Atlantic Anomaly region and in the

North and South Aurora belts. Probability of false detections depends on the space weather, rising during magnetic storms.

Due to the VIIRS sensor design it is improbable that particles will simultaneously hit detectors for the same ground pixel in several spectral bands. Thus simultaneous observation of hot spots in multiple infrared bands and the visible DNB band can confirm the presence of an IR emitter on the ground. Figure 3 illustrates the difference in error rate of the single- and multiband detectors. The left map shows all single-band detections in the South Atlantic Anomaly region in the period of high magnetic activity in July 2012. The right map shows noise reduction result using the multiband detector. Local maximum observed above detection threshold in band M10 is considered to be a real IR source if and only if it detected above the noise level at least in one more spectral band.

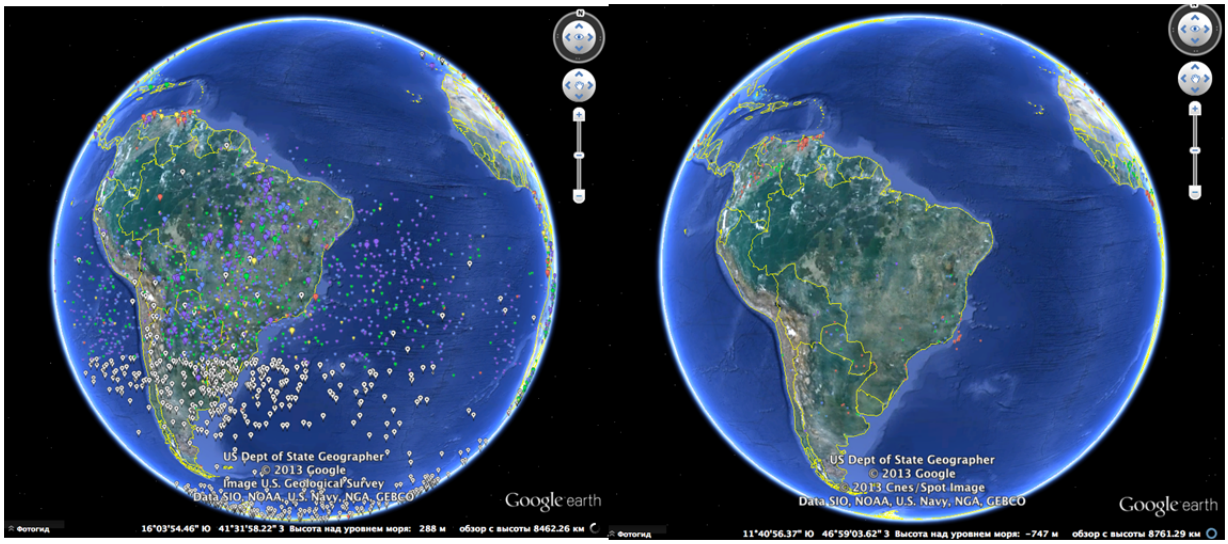

Figure 3. Difference in error rate of the single- and multiband detectors. (left) Single-band detections in the South Atlantic anomaly region. (right) Noise reduction result using multiband detector.

2.4 Filtering to remove bow-tie duplications

To filter out the overlapping pixels lit by the same IR point source, the source location can be given as a local maximum of the brightness values, shown by red plus in Figure 4. There exist two definitions of local maximum, one of them is strict and requires the local maximum value to be strictly greater than neighbor pixel values. Another definition is less restrictive and requires the local maximum to be greater or equal than its neighbors. Applying the strict definition will result in undesirable suppression of flat plateaus with the equal brightness. To search for the local maxima in the M10 channel image we use a modified version of the fast algorithm reported

to use less than two comparisons per pixel [6]. Modifications of the algorithm include change from the strict to non-strict local maxima definition and correction for the satellite projection geometry called bow-tie effect.

Geometry of the VIIRS moderate resolution infrared M-channels is shown in Figure 5. The VIIRS radiometer simultaneously scans 16 lines of pixels, shown in Figure 3 as Scan 1 through Scan 4. These 16-line scans do not overlap at nadir, but they suffer from the 50 % overlap at the edges of image. As a result, for relatively small scan angles (close to nadir) the same IR source can be observed at the adjacent lines of the M10 image, as shown in Figure 6. In the outer portions of scans, single point source on the Earth surface can be observed in the same column but at two different lines of the M10 data several pixels apart.

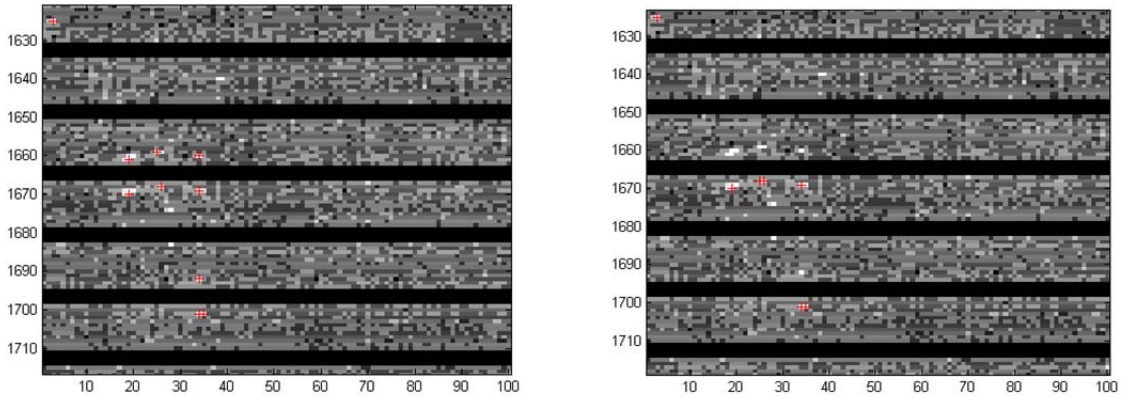

Figure 4. Result of the bow-tie correction in the local maxima search algorithm. **(left)** All local maxima brighter than noise threshold are marked by red pluses. **(right)** Half of them are suppressed after the bow-tie correction.

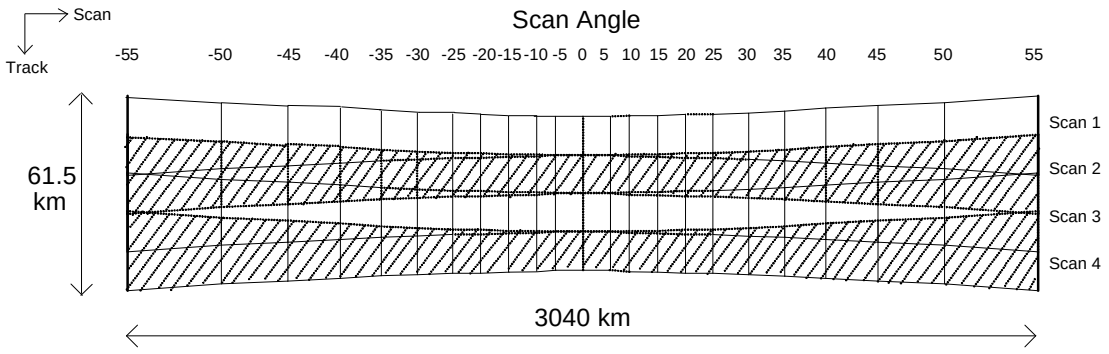

Figure 5. Geometry and overlap (bow-tie) of the VIIRS 16-line scans for medium resolution infrared M-bands.

The result of the bow-tie correction in the local maxima search algorithm at the edge of the M10 image is shown in Figure 4. In the left fragment all local maxima brighter than the noise threshold are marked by red pluses. In the right fragment half of them is suppressed after the bow-tie correction. For the above image of the Persian Gulf area the local maxima search gives 319 IR sources before and only 290 sources after bow-tie correction.

2.3. Fitting Planck curve to multispectral observations

Temperature and radiant heat intensity of the detected IR sources can be estimated by simultaneous fitting of the Planck black body spectral curve (equation 1) to the observed radiances of all VIIRS infrared M-channels, which are above noise level. Here we assume that spectra of the high-temperature flares at night are ideal black body. Under this assumption the emissivity scaling factor ε in the Planck formula (equation 1) becomes a proxy for the proportion of the pixel footprint which holds the IR source. This makes it possible to calculate source sizes.

Figure 8 illustrates the fit of the Planck curve to the observed radiances for a gas flare. A non-linear fitting algorithm searches for the optimal values of the flare temperature T and emissivity scaling factor ε to minimize the sum of square differences between the model and the observed

radiances at the central wavelengths of the M-bands. In that particular case the IR source emits signal above noise levels in the DNB, M7, M8, M10 and M12 bands, but it was not detected by the M13 band. In the Figure 6 the M-band radiance values used for the Planck curve fitting are shown in red. The observed but not used values are shown in blue. The fitted Planck black body curve is shown as a blue line. For band M12 we show in red the difference between the observed value and the background in the local window centered at the IR source location under study (see 2.2).

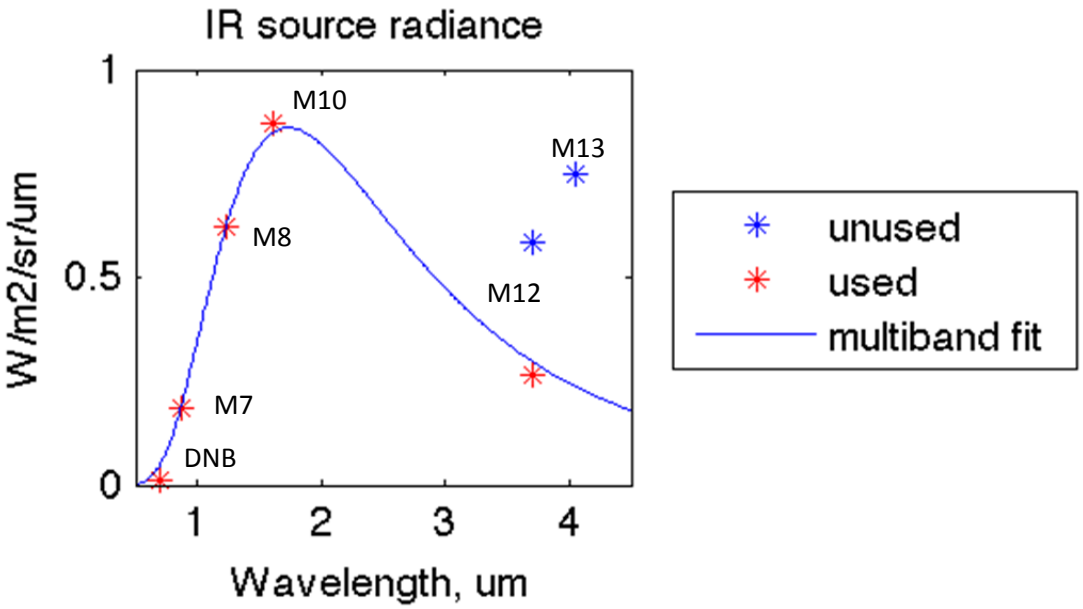

Figure 6. Radiances observed for a gas flare and the resulting Planck curve.

Given emissivity scaling factor and temperature, the radiant heat intensity from a small flat black body surface radiating out into a half-sphere can be derived using Stefan-Boltzmann Law:

$$I(T) = P(T)/A = \int_0^\infty R(\lambda, T)d\lambda \int d\Omega = \epsilon\sigma T^4 \qquad (2)$$

where $I(T)$ is the radiant heat intensity (W/m^2) from the pixel containing the detected IR source, $P(T)$ is the total radiant heat of the flare (W), A (m^2) is the pixel footprint, $R(\lambda, T)$ is the spectral radiance (W/m^2/sr/um, see (1)), ϵ is the emissivity scaling factor, T is the absolute temperature of the black body (K), $d\Omega$ is infinitesimal solid angle, and σ is Stefan-Boltzmann's constant. To

derive further the total radiant heat $P(T)$ (W) and the footprint area S (m^2) of the IR source, we multiply the radiant heat intensity and the scaling factor by the pixel footprint area:

$$P(T) = I(T) \times A$$
$$S = \epsilon \times A \tag{4}$$

For example, the estimated parameters of the flare with the spectrum in Figure 8 are T = 1673 K, $I(T) = 7.12$ W/m^2, $P(T) = 6.72$ MW, S = 15 m^2. The distance from the actual flare found on the Google Earth daytime image to the center of the M10 pixel that contains the flare is 300 m. Location and parameters of the detected flare are shown in Figure 7.

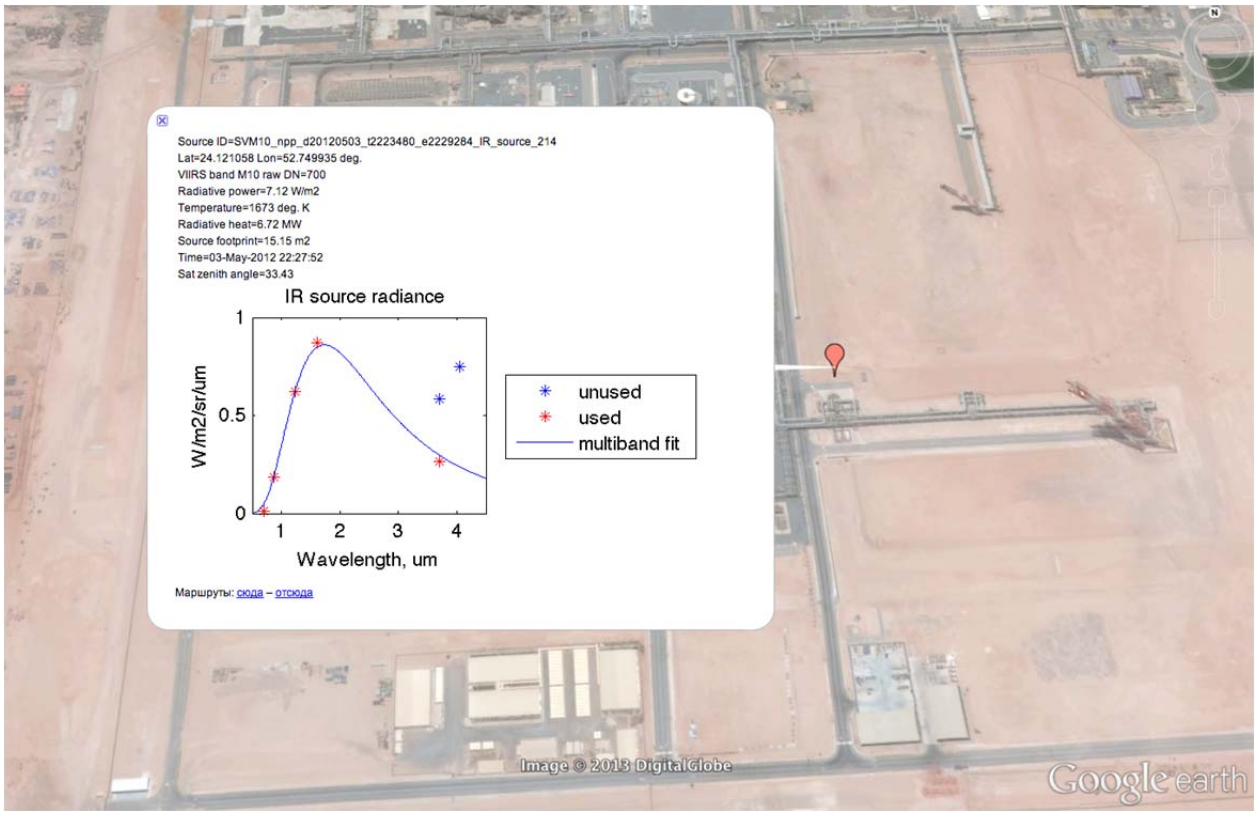

Figure 7. Example of results present in the KMZ file for a gas in the Persian Gulf area.

3. Results

Nocturnal detection of the short-wave IR radiated from combustion sources is performed at the NOAA National Geophysical Data Center (NGDC) in Boulder nightly on a regular basis using global coverage UTC day VIIRS dataset received from the NOAA Comprehensive Large Array Stewardship System (CLASS) [7]. VIIRS dataset comes from CLASS as a set of HDF5 formatted files divided by the 4 min of the satellite flight time for each satellite band. Multiband IR source detection first is performed separately for each of the 4 min flight time data aggregates. At the last step of the procedure detection the results for all the 4 min aggregates are merged together into a single table containing a global set of the nocturnal short-wave IR combustion sources for the given UTC day. Typical number of IR source detections per night is around 15,000.

Detection results are presented to the end user in two forms: as a CSV formatted table and as a KML formatted vector map. The CSV table has entries for all the M10 pixels with radiance above the noise level THR_{M10} such as IR source location and time stamp, M-channel radiances, satellite position, cloud coverage, etc. The KML map shows locations of all the multiband detections, i.e. the M10 image local maxima collocated with a hot spot in another M or DNB band. Using the KML file, the combustion sources can be shown on the Google Earth (or Maps) with the "balloon" type placemarks of different size and color. The color and size legend for the Google Earth display of the detection vector map is presented in Table 2. The Google Earth screenshot with the global detections map for 29 January 2013 is shown in Figures 8.

Table 2. Color and size legend for Google Earth display of the IR sources

Size legend		**Color legend**	
Size	**Radiant heat**	**Color**	**Temperature**
large	P(T) > 10 MW	red	$T > 1600$ K
medium	1 MW < P(T) < 10 MW	yellow	1400 K < T < 1600 K
small	P(T) < 1 MW	green	1200 K < T < 1400 K
		blue	1000 K < T < 1200 K
		purple	$T < 1000$ K

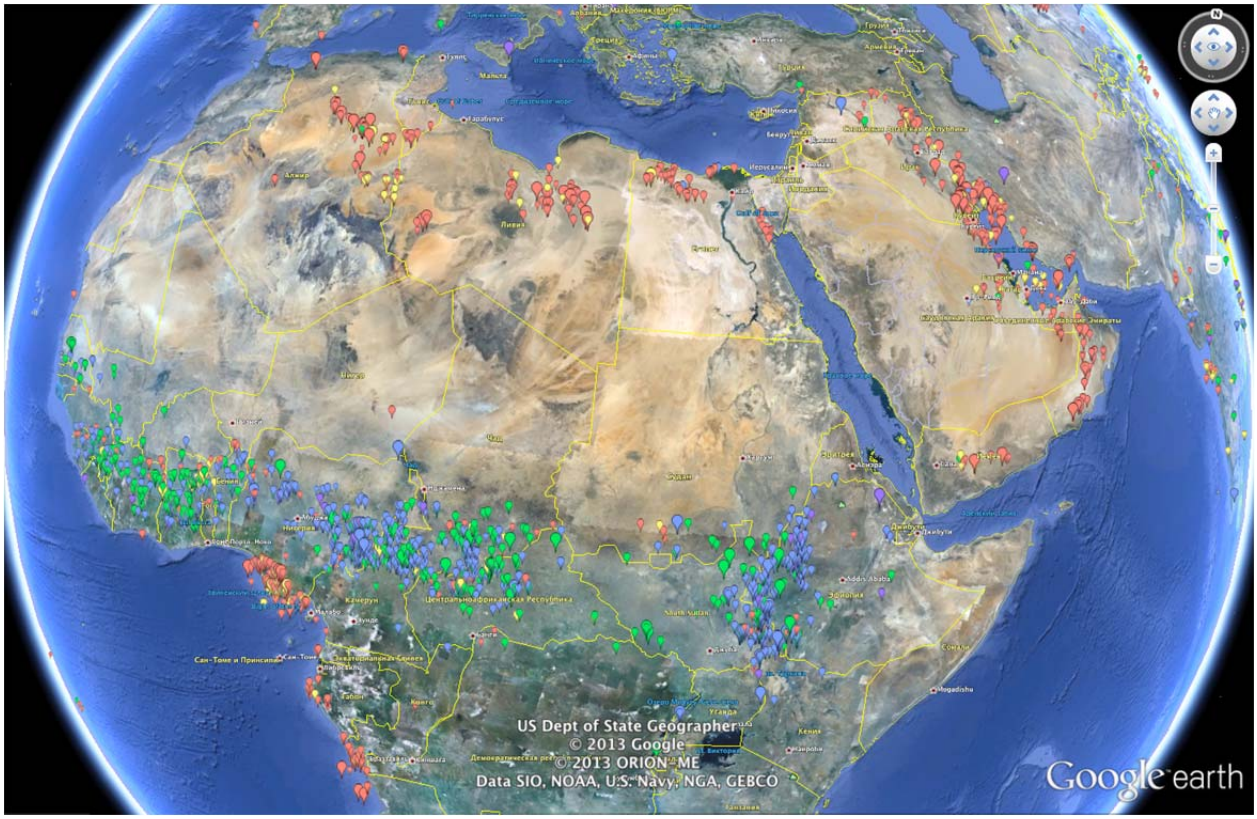

Figure 8. A screenshot from Google Earth with the nightly global map of the short-wave IR source detections.

Color legend of the Google Earth map helps to distinguish low-temperature biomass burning from the high-temperature gas flares and open lava lakes. For example, in Figure 8 it helps to highlight oil and gas exploration regions in Nigeria, Morocco, Algeria, Egypt and Persian Gulf from the savanna fires in Sub-Saharan Africa.

Both CSV tables and KML maps with the nightly detections of combustion sources are in open access and can be downloaded from the NGDC web page [8].

4. Conclusions

Multi-band detection of IR combustion sources with data from the new NPP satellite gives estimates of the flare temperature, size and radiant heat. Using data from visible DNB and infrared M7, M8, M10, M12 and M13 of the VIIRS sensor it is possible to detect fires and heat sources on the night side of the Earth with temperature between 600 K and 3000 K and with the minimal footprint around 1 m^2. Running global operational detector at NOAA NGDC results in about 15,000 IR sources per night. Detection results are openly available from the NGDC web server.

Acknowledgments

This research has been funded by NOAA's JPSS Proving Ground program.

References and Notes

1. Wooster, M.J.; Roberts. G.; Perry, G.L.W.; Kaufman, Y.J. Retrieval of biomass combustion rates and totals from fire radiative power observations: FRP derivation and calibration relationships between biomass consumption and fire radiative energy release. JGR, 2005, D24311

2. Elvidge, C.D.; Ziskin, D.; Baugh, K.E.; Tuttle, B.T.; Ghosh, T.; Pack, D.W.; Erwin, E.H.; Zhizhin, M. A Fifteen Year Record of Global Natural Gas Flaring Derived from Satellite Data. Energies, 2009, 2(3), 595-622

3. Dozier, J. A Method for Satellite Identification of Surface Temperature Fields of Subpixel Resolution. REMOTE SENSING OF Environment, 1981, 11, 221-229

4. Matson, M.; Dozier, J. Identification of Subresolution High Temperature Sources Using a Thermal IR Sensor. Photogrammetric Engineering and Remote Sensing, 1981, 47, pp. 1311-1318

5 Justice, C.; Giglio, L.; Boschetti, L.; Roy, D.; Csiszar, I.; Morisette, J.; Kaufman, Y. MODIS Fire Products (Version 2.3, 1 October 2006). Algorithm Technical Background Document

6. Pham, Tuan Q.. Non-maximum Suppression Using Fewer than Two Comparisons per Pixel. 12th International Conference, ACIVS 2010, Sydney, Australia, December 13-16, 2010, Proceedings, Part I, pp. 438-451.

7. NOAA Comprehensive Large Array Stewardship System (CLASS). URL http://www.class.ngdc.noaa.gov (accessed on 29 January 2013)

8. NOAA NGDC web page with the nightly global IR source detection results. URL http://www.ngdc.noaa.gov/dmsp/data/viirs_fire/viirs_html/download_viirs_fire.html (accessed on 29 January 2013)